ACS APPLIED MATERIALS & INTERFACES

RESEARCH ARTICLE

www.acsami.org

Photochemical Stabilization of Terthiophene and Its Utilization as a New Sensing Element in the Fabrication of Monolayer-Chemistry-Based Fluorescent Sensing Films

Taihong Liu, Liping Ding,* Gang He, Yang Yang, Wenliang Wang, and Yu Fang*

Key Laboratory of Applied Surface and Colloid Chemistry of Ministry of Education, School of Chemistry and Materials Science, Shaanxi Normal University, Xi'an 710062, P. R. China

Supporting Information

ABSTRACT: To improve the photochemical stability of α-terthiophene (3T) in air, we purposely introduced a naphthalene unit into its conjugated backbone, resulting in a fluorescent compound, 5-(1-naphthyl)-2,2′:5′,2″-terthiophene (NA-3T). The compound was further employed as a sensing element for the fabrication of a monolayer-chemistry based fluorescent sensing film. It was demonstrated that the fabricated film is highly sensitive and selective to the presence of picric acid (PA). The detection limit was found to be 3.2×10^{-7} mol/L. The high sensitivity of the film to PA has been attributed to the specific binding of the film to the analyte because of proton transfer from PA to the amino group in the spacer, which is in accordance with the static nature of the quenching as revealed by fluorescence lifetime measurements. Further experiments demonstrated that the sensing process is fully reversible and free of interference from common organic solvents, acids and bases, etc. In addition, the film is stable, at least, within half a year provided it is properly preserved. More importantly, the present work makes it possible to use oligothiophenes as a new class of sensing elements, which may combine the advantages of conjugated polymers or oligomers and those of fluorescent compounds of low-molecular masses. This effort enlarges, definitely, the applications of oligothiophenes and the space for creating monolayer-chemistry based fluorescent sensing films.

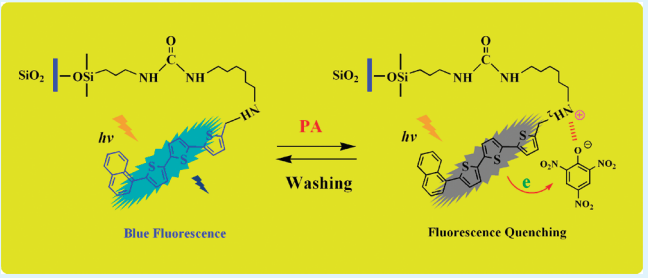

KEYWORDS: monolayer-chemistry, film sensor, naphthyl-capped terthiophene, fluorescence quenching, picric acid

1. INTRODUCTION

π-Conjugated oligothiophene and its derivatives with well-defined structures possess sophisticated electronic and optical properties, and are frequently employed as central players for creating various optoelectronic active molecular devices, e.g., organic light-emitting diodes (OLEDs), transistor circuits, optical memories, optical modulators, and chemical and biochemical sensors, etc.[1−3] Considerable efforts have been devoted to the development of chemo- and biosensors based on oligothiophenes bearing appropriate recognition units that are able to provide optical and electronic response in the presence of a large variety of analytes such as cations and anions.[4−6] However, most of the reported oligothiophene-based chemo- or biosensors are solution-used. In comparison, surface-confined sensors have advantages in terms of reuse-ability, ease to be made into devices, and no contamination to analytical systems. Among various approaches of immobilizing fluorophores onto the inorganic solid surfaces, self-assembled monolayers (SAMs) with functional termini represents a more promising one to fabricate fluorescent sensing films. This is because the formation of SAMs on the surface and the attachment of fluorophores to the functional ends of SAMs are chemical linkage, which provides high stability and ensures the obtained films to perform in harsh environments.[7−9] On the other hand, the fluorophores are well-defined on the surface on the molecular level and can be directly exposed to the test solution, which in turn endows the film with fast response to the analytes.

Using this methodology, our group has immobilized a certain number of polycyclic aromatics such as pyrene, dansyl, and anthracene on functional SAMs to prepare various fluorescent sensing films. These sensing films have shown sensitive and selective responses to different analytes either in gas or in solution.[9] We have also extended this method to fabricate oligothiophene-functionalized SAM sensors, where oligothiophene with three or four repeat units were immobilized on an amino-terminated SAM.[10,11] We found that these oligothiophene-functionalized SAM films have poor stability when exposed to UV light. Actually, this is a common issue in using oligothiophene and polythiophene to fabricate devices. These devices are reported to have inadequate thermal and photochemical stability and show rapid device-performance degradation, which should be related to the relatively large energy gap of these materials as well as the energy level of their highest occupied molecular orbital (HOMO).[12−14] Surprisingly, the exposure to HCHO gas can generate a new fluorescence emission of our

Received: January 17, 2011
Accepted: March 30, 2011
Published: March 30, 2011

dx.doi.org/10.1021/am2000592 | ACS Appl. Mater. Interfaces 2011, 3, 1245–1253

oligothiophene-functionalized films after they are totally photochemically bleached.[10,11] Although these films can be explored as HCHO sensing films, the issue of poor photochemical stability severely restricts the application of oligothiophene-functionalized fluorescent sensing films. The functionalization of oligo- and polythiophenes in its α- and β- position with a variety of aromatic moieties have been reported to be used to adjust the energy gap between the lowest unoccupied molecular orbital (LUMO) and the HOMO of each of the compounds to increase their photochemical stabilities.[14−16] This method has been widely applied in fabricating oligothiophene-functionalized devices in the area of OLEDs and field-effect transistors. However, to the best of our knowledge, oligothiophene bearing aromatic substituents are rarely used as sensing elements in the fabrication of monolayer-chemistry based fluorescent sensing films.

The object of the present work is to fabricate oligothiophene-functionalized SAM films with enhanced photochemical stability, and thereby 5-(1-naphthyl)-2,2′:5′,2″-terthiophene (NA-3T) was specially synthesized and immobilized on a glass-supported isocyanate-terminated SAM. The introduction of naphthalene into the conjugated backbone of the oligothiophene is expected to improve its photochemical stability by adjusting its HOMO energy level and the energy gap between its HOMO and LUMO. The photochemical stability of this NA-3T was examined both in air and in aqueous solution and the sensing ability of this film was also investigated.

2. EXPERIMENTAL SECTION

2.1. Reagents and Materials. The silane coupling agent, (3-isocyanatopropyl)triethoxysilane (ICPTES, TCI, >95.0%), was used directly without further purification. THF and toluene were distilled over sodium in the presence of benzophenone under nitrogen atmosphere before use. Nitroaromatics (NACs), including PA (2,4,6-trinitrophenol), TNT (2,4,6-trinitrotoluene), DNT (2,4-dinitrotoluene), and NB (nitrobenzene), are of analytical grade and used directly without further purification. All other reagents were analytically pure. Water used throughout was deionized and then double distilled. Glass substrates used in the experiment for fabrication of SAM films were microscope slides with size of ∼0.9 cm × 2.5 cm.

2.2. Fluorescence Measurements and Characterization Methods. Fluorescence measurements were performed at room temperature on a time-correlated single photon counting fluorescence spectrometer (Edinburgh Instruments FLS 920) with a front face method.[17−19] The fabricated film was inserted into a quartz cell with its surface facing the excitation light source. The position of the film was kept constant during each set of measurements. The ^{1}H NMR, ^{13}C NMR spectra of the samples were obtained on a Bruker Avance 300 MHz NMR spectrometer. The mass spectra were acquired in ESI positive mode using a maXis UHR-TOF Mass Spectrometers (Bruker, USA). Pressed KBr disks for all the powder samples were used for the transmission infrared spectroscopy measurements and their FTIR spectra were measured with a Bruker Tensor 27 FTIR spectrometer. X-ray photoelectron spectroscopy (XPS) measurements were carried out on a Thermo Scientific Escalab 250Xi photoelectron spectrometer. The contact angles of the film surfaces were measured on a video-based contact angle measuring device SCA20. UV−vis spectra of solution samples were recorded on a spectrophotometer (Lambd 950, Perkin-Elmer, USA). Analysis of C and H was conducted on a PerkinElmer 2400 CHN elemental analyzer. The structures of the HOMO and the LUMO states of the investigated compounds were calculated with the help of theoretical calculations, in the framework of the density functional theory (DFT) at the B3LYP/6-311G(d,p) level in a suite of Gaussian 03 programs.

2.3. Preparation of 5-Formyl-5″-(1-naphthyl)-2,2′:5′,2″-terthiophene (NA-3T-CHO). The oligothiophene derivative NA-3T was specially designed by introducing naphthalene moieties to the α-position of terthiophene to provide a fluorophore with higher photochemical stability. The derivative was synthesized by using a Grignard coupling reaction in a good yield according to a literature procedure.[12,20] Then, this naphthyl-capped terthiophene was further modified with an aldehyde group so that it can be further derived with amino groups. A literature method was slightly modified and employed for the synthesis of NA-3T-CHO:[10,21] 1.2 mL of $POCl_3$ (13.0 mmol) was slowly added to 50 mL of DMF at 0 °C. The solution was stirred for 30 min under N_2 atmosphere. Then, 50 mL of DMF solution of NA-3T (3.74 g, 10.0 mmol) was added dropwise to the above solution. After the addition, the yellow solution was stirred for another 30 min at room temperature, and then at 80 °C for 4 h. The color of the system changed into a dark red solution at the end of the reaction. Finally, the solution was cooled to room temperature, and added with 100 mL of cold saturated aqueous solution of sodium acetate. A dark red precipitate was produced, filtered, and washed repeatedly with water. The crude product was purified by chromatography on silica gel with dichloromethane/*n*-hexane (3:1, V/V) as the eluent. The purified NA-3T-CHO was collected as a red solid with a yield of 62.2% (∼2.5 g); FTIR (KBr): 3053, 2798, 1652, 1443, 1390, 1217, 1046, 858, 788, 665, 555, 475 cm^{-1}. ^{1}H NMR (δ ppm, 300 MHz, $CDCl_3$): 9.87 (s, 1H), 8.29 (1H), 7.92−7.87 (2H), 7.68 (1H), 7.59−7.51 (4H), 7.31−7.30 (3H), 7.20−7.18 (2H). ^{13}C NMR (δ ppm, 75 MHz, $CDCl_3$): 182.38, 146.83, 141.62, 139.16, 137.32, 134.53, 133.94, 131.70, 131.66, 128.83, 128.48, 128.36, 128.11, 127.00, 126.69, 126.26, 126.19, 125.52, 125.30, 124.77, 124.65, 124.59, 124.07. Anal. Calcd. for $C_{23}H_{14}OS_3$: C, 68.62; H, 3.51; Found: C, 68.37; H, 3.64. MS (*m*/*z*): calculated [$(M+Na)^+$]: 425.0099, Found: 425.0102.

2.4. Synthesis of *N*-5-(5″-(1-Naphthyl)-2,2′:5′,2″-terthiophene)-1,6-hexanediamine (NTHA). The amino derivative of NA-3T-CHO, NTHA, was prepared to react with the isocyanate-terminated SAM to realize its covalent attachment on the solid surface. The synthesis procedure goes as follows: 1,6-hexanediamine (2.32 g, 20.0 mmol) was added to 30 mL of methanol and stirred rapidly under reflux with a nitrogen blanket. NA-3T-CHO (1.00 g, 2.49 mmol) was dissolved in 100 mL $CHCl_3$/MeOH (1:1, V/V) and added dropwise to the stirred solution over a period of 6 h. A yellow solution was observed and the mixture was refluxed for additional 10 h. Once the solution was cooled to room temperature, $NaBH_4$ (0.38 g, 10.0 mmol) was added and then stirred at room temperature overnight. The solvent was removed by rotary evaporation to give an oily orange residue which was partitioned between 100 mL of $CHCl_3$ and 25 mL of 1.0 mol/L NaCl solution. The organic layer was further washed with water several times and dried over anhydrous $MgSO_4$ overnight. The solid obtained after evaporating the solvent was recrystallized twice from methanol/*n*-hexane to give NTHA as a sticky orange solid (0.85 g, 68.0%). FTIR (KBr): 3423, 2929, 2789, 1589, 1508, 1441, 1392, 1219, 1043, 1000, 855, 790, 475 cm^{-1}. ^{1}H NMR (δ ppm, 300 MHz, $CDCl_3$): 8.30 (1H), 7.85−7.87 (2H), 7.60−7.51 (4H), 7.24−7.02 (5H), 6.82 (1H), 3.96 (2H), 2.67−2.54 (4H), 1.44−1.25 (11H). ^{13}C NMR (δ

Scheme 1. Synthesis of NA-3T-CHO and NTHA, and Schematic Representation of the Fabrication of the NA-3T-Functionalized Fluorescent Film

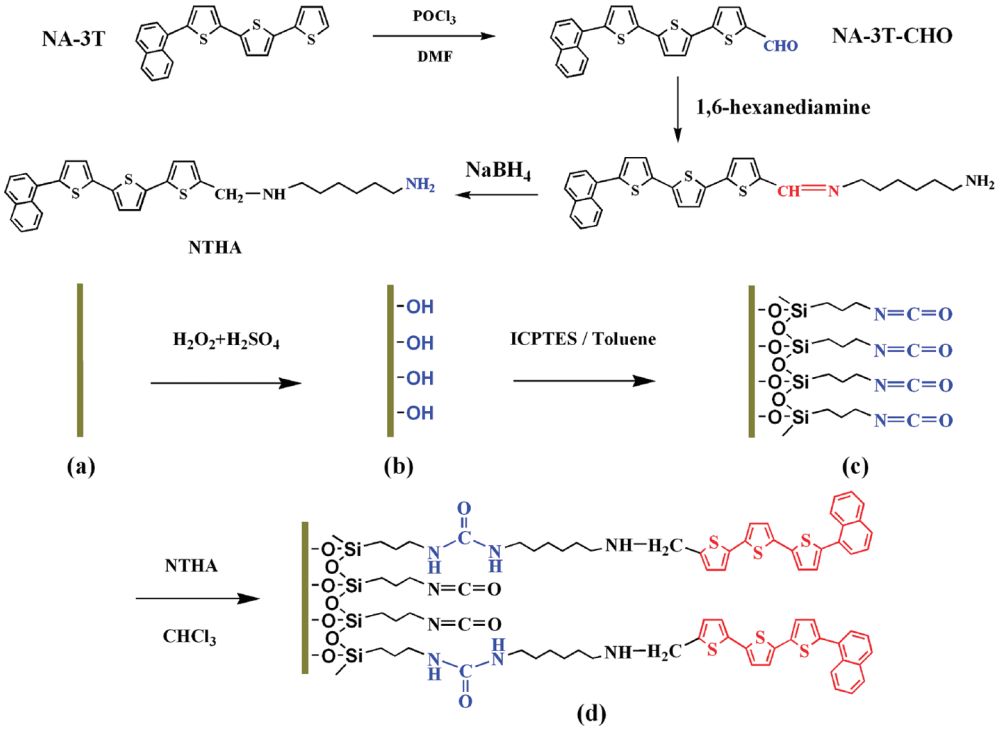

ppm, 75 MHz, $CDCl_3$): 144.25, 140.85, 137.42, 136.71, 135.94, 135.77, 133.95, 131.98, 131.68, 128.60, 128.43, 128.18, 128.04, 126.59, 126.12, 125.65, 125.40, 125.30, 124.27, 123.95, 123.85, 123.23, 49.17, 48.71, 42.17, 33.70, 30.05, 27.19, 26.84. MS (m/z) for $C_{29}H_{30}N_2S_3$: calculated $[(M+1)^+]$: 503.1649, Found: 503.1643.

2.5. Activation and Silanization of the Glass Wafer Surfaces. The clean glass wafers were treated in a boiling "piranha solution" (30% H_2O_2/98% H_2SO_4: 3/7, V/V) at 98 °C for 1 h. (***Caution:*** *piranha solution is a very strong oxidant and reacts violently with many organic materials, it must be handled with extreme care.*) Then, the wafers were rinsed thoroughly with plenty of water and dried with N_2 flow. After the treatment, the wafers were immersed in a warm (50 °C) toluene solution of the isocyanate-terminated silane, ICPTES, (0.67%, V/V) containing a trace amount of water for 12 h. The ICPTES-modified wafers were washed successively with toluene and CH_2Cl_2 for several times to ensure that they are free of unbound ICPTES.[22,23]

2.6. Chemical Coupling of NA-3T on the Glass Wafer Surface. The ICPTES-modified wafers were further macerated into a solution of 0.1 g NTHA in 30 mL $CHCl_3$ under reflux for 6 h. The isocyanate-terminated SAMs on the glass surface were expected to react with NTHA. To remove unreacted NTHA, the wafers were extracted with CH_2Cl_2 in a Soxhlet extractor for 3 h. After the extraction, the wafers were further rinsed with plenty of methanol, acetone and water, successively. The synthesis route of NA-3T-CHO and NTHA and the fabrication process were schematically shown in Scheme 1.

3. RESULTS AND DISCUSSION

3.1. Characterization of the NA-3T-Functionalized Film. The immobilization of the indicator fluorophore, NA-3T, on the support substrate is a crucial step in the preparation of fluorescent SAM sensors. Silanization with a specially chosen agent is one of the most commonly used approaches to introduce functional groups onto glass wafer surfaces.[24] By employing this technique, the "piranha solution"-activated glass wafer surfaces were treated with ICPTES to obtain isocyanate-terminated surfaces. It is believed that the isocyanate group should react with amine groups of NTHA, and then realize the covalent attachment of the fluorophore to the surface and form a stable fluorescent SAMs.

Figure 1. Static contact angles (θ) (H_2O) for various glass wafer surfaces, where the meanings of a, b, c, and d are the same with those explained in Scheme 1.

Contact angle (CA) measurement is a simple but efficient way to characterize surface properties about the structure and composition of surface and then reflects surface functionality. The static contact angles with water for the surfaces at different coupling stages are shown in Figure 1. It can be seen that the activation process made the contact angle of glass wafer surface decrease from 27.5 ± 1.1° to 10.5 ± 0.4°, indicating that more hydroxyl groups were generated after this process, which should be favorable for the silanization of the surface. Silanization process decreased the wettability of the surface dramatically as revealed by the distinct increase of the CA values from 10.5 ± 0.4° to 73.0 ± 0.4°, in support of successful introduction of the hydrophobic isocyanate-chains onto the substrate surfaces. Introduction of NTHA decreased the angle to

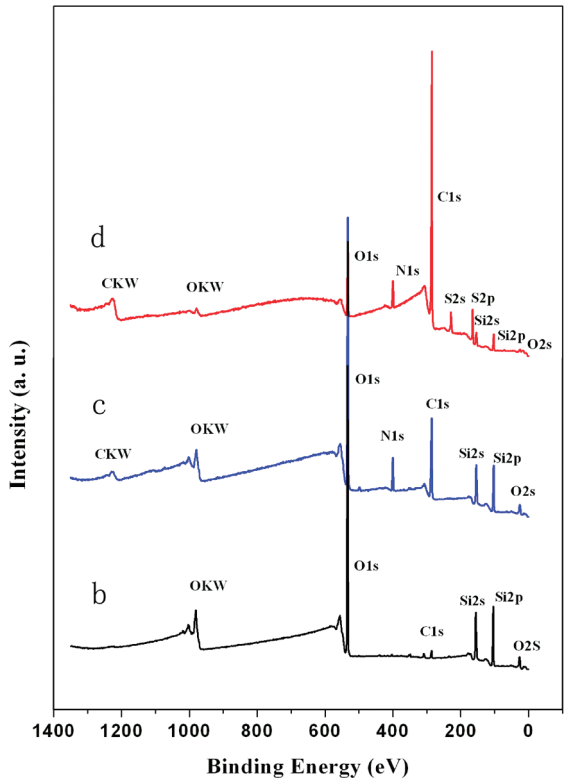

Figure 2. XPS traces of the films, where the meanings of b, c, and d are the same as those explained in Scheme 1.

50.3 ± 0.5°, suggesting that the surface became less hydrophobic. This may be due to the introduction of the hydrophilic carbamido groups and amino groups onto the surface in the process of attaching NTHA. These results were consistent with the expectation from the chemical compositions of the glass wafer surfaces as shown in Scheme 1.

Chemical coupling of NA-3T on the glass wafer surface was further confirmed by XPS measurements. Figure 2 depicts the XPS spectra of the glass wafers with different surface compositions and structures. Compared with the activated glass wafer, the XPS spectrum of the ICPTES-modified glass wafer surface is characterized by two N1s signals, appearing at 399.6 and 401.3 eV, indicating the presence of nitrogen-containing molecules on the substrate surface in accordance with the chemical modification. It can be also seen that the signal of C1s (284.6 eV) became much stronger on the isocyanate-terminated surface, a direct evidence for the successful coupling of the organic silane agent. As expected, immobilization of NA-3T made the signal of C1s become even stronger, and meanwhile the specific signal of S2p (170.1 eV) appeared, which is, of course, originated from the surface-bound NA-3T moieties. Therefore, it was believed that the fluorescent NA-3T was successfully immobilized on the glass surface. From calculating the ratio of different elements shown in the XPS spectra, the average loading density of NA-3T on the surface was determined to be about 32.5%, which is suitable for sensing.[10,25]

3.2. Fluorescence Properties of α-Terthiophene and Its Derivatives. The fluorescence excitation and emission spectra of 3T, NA-3T, and NA-3T-CHO in dilute CH_2Cl_2 solution were investigated to evaluate the effect of the naphthalene moieties on the photochemical properties of oligothiophene. The spectra are shown in Figure 3 and the main optical properties are depicted in

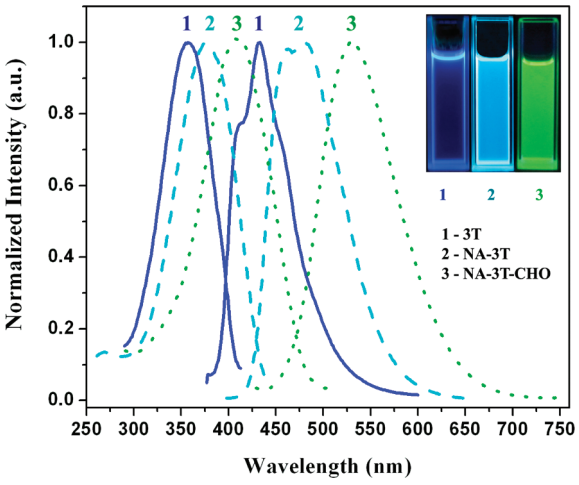

Figure 3. Normalized fluorescence excitation and emission of oligothiophene and its derivatives in their dilute CH_2Cl_2 solutions and the inset is the color of these solutions under ultraviolet lamp (λ = 365 nm).

Table 1. It shows that the maximal excitation wavelength of NA-3T is at 377 nm, and the emission maximum is at 481 nm with a shoulder located around 461 nm with bright green color. The emission maxima have shifted to the longer wavelengths in comparison with the original oligothiophene (3T, 433 nm) and naphthalene (NA, 335 nm).[26] The NA-3T-CHO has the same main chain as NA-3T does but they have different chemical substituent at one of their edges. NA-3T-CHO exhibits red-shifts and structure-less spectra, emitting light in the yellow spectral region. While NTHA has a single absorption maximum at 384 nm and the same fluorescence emission spectrum at 484 nm as NA-3T does (c.f. Figure S1 in the Supporting Information), which indicates that they have the same chromophore unit. These results suggest that no single naphthalene or 3T emission band could be observed from the emission spectra of the derivatives, indicating a conjugation occurs between the naphthalene moieties and the thiophene chain. A nonperpendicular structure was believed being adopted in the NA-3T as a dihedral angle ca. 55.85° was calculated existing between the thiophene unit and the terminal naphthalene ring (c.f. Figure S2 in the Supporting Information). The extension of the π-conjugation between these two moieties thereby allows for delocalization throughout the molecular via the carbon−carbon bond.[27,28] The influence of substituents on the molecular orbital is also investigated. The frontier molecular orbitals of 3T and its derivatives calculated by DFT calculations are presented in Figure 4. It shows that both HOMO and LUMO are π-type orbital. The HOMO level of NA-3T (−5.32 eV) is a little higher than that of 3T (−5.37 eV), suggesting the introduction of the naphthyl groups contributes to a stronger electron-donating ability for NA-3T.[29,30] Meanwhile, NA-3T should have better stability as its HOMO energy level is lower than the oxidation threshold (ca. −5.2 eV).[31,32]

The calculated energy gap (E_g(cal.)) and the optical band gap (E_g(expl.)) are also shown in Table 1. The data for E_g(cal.) was obtained by a DFT method and it shows that the energy gap decreases along the order of 3T, NA-3T, and NA-3T-CHO. The optical band gaps of these small molecules were derived from the absorption edges of the UV−vis spectra and it shows a similar decreasing trend in the range of 3.21−2.73 eV. The calculated energy gaps appear to be systematically higher than the optical band

Table 1. Optical Properties of Oligothiophene and Its Derivatives

compds	Ex (nm)[a]	Em (nm)[a]	Stokes' Shift	HOMO[b]	LUMO[b]	E_g (expl.)[c]	E_g (Cal.)	ΔE_{H-L} (eV)[d]
3T	357	433	76	−5.37	−1.95	3.18	3.21	3.42
NA-3T	377	461, 481	104	−5.32	−2.00	3.00	3.02	3.32
NA-3T-CHO	419	532	113	−5.60	−2.63	2.69	2.73	2.97

[a] Measured in CH_2Cl_2. [b] Calculated by B3LYP/6-311G(d,p). [c] Calculated by UV−vis spectra. [d] ΔE_{H-L} = LUMO−HOMO.

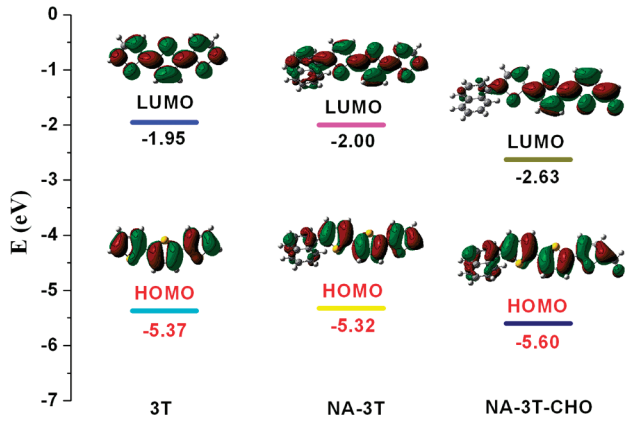

Figure 4. Molecular orbital contours of the HOMO and LUMO for 3T and its derivatives at B3LYP/6-311G(d,p) level.

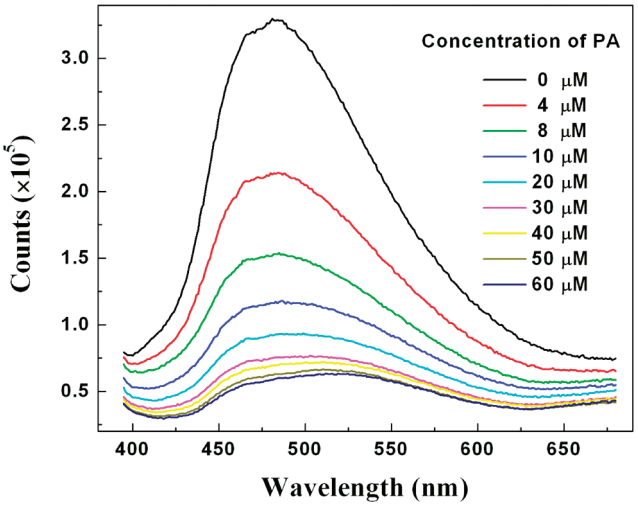

Figure 5. Steady-state emission spectra of NA-3T-functionalized film in response to various concentrations of PA solution.

gaps, which is presumably because of the fact that the calculations were performed in vacuum. The position and shape of the high energy $\pi-\pi^*$ transitions (c.f. Figure S3 in the Supporting Information) reflect the interplay of molecular structure and substitutions. From the absorption and emission spectra discussed above, it is clear that the excitation energy (band gap) of oligothiophenes decreases for a system with increasing conjugation.[3,30]

3.3. Fluorescence Properties of NA-3T-Functionalized SAM Films. The fluorescence properties of the NA-3T-functionalized SAM films were also investigated under different conditions. It is found that the SAM films in water display strong fluorescence emission with a peak centering at 482 nm when it is excited by radiation of 381 nm, which suggests the fluorescence properties of

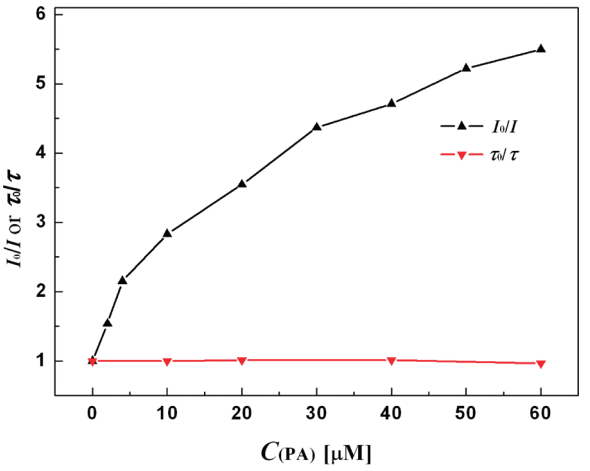

Figure 6. Plot of I_0/I or τ_0/τ as a function of PA concentration.

NA-3T was restored when it is localized on the substrate surface. The effect of oxygen on the fluorescence properties of the surface-supported NA-3T was examined by exposing the film in the air and recording the fluorescence intensity when excited at 381 nm. The fluorescence emission of these films in air does not decrease significantly along with increasing the scanning numbers as observed in our previous studies, indicating that the photochemical stability of oligothiophene is indeed improved with naphthalene on the α-position even when immobilized on solid surface (c.f. Figure S4 in the Supporting Information).[10] The leaking issue was also examined by investigating the fluorescence emission of the solvent, in which the functionalized film had been immersed for 3 h. No evidence of existence of free NA-3T in the solvent was observed. It could be attributed to the covalent attachment of NA-3T on the surface, and thereby, the leaking of NA-3T from the glass plate surface was negligible. These results suggest that the modified oligothiophene-functionalized films can be used for exploring their fluorescent sensing applications.

3.4. Fluorescence Quenching and Lifetime Measurements. The sensing properties of this NA-3T-functionalized SAM films were explored by fluorescence quenching and fluorescence lifetime measurements. As is well-known, NACs are effective fluorescence quenchers to most fluorophores. The fluorescence emission of the present film was recorded in the presence of a series of NACs to evaluate the responses of the film to them. The testing procedure goes as follows: the film was first adhered to one inner-side of a quartz cell. Then, 2.5 mL of water was added into the cell. Finally, the spectra were recorded when the fluorescence intensity kept being stable after each injection of the NACs or interferents into the cell. As expected, all the NACs quenched, with different efficiency, the emission of the NA-3T-functionalized films. Among all the NACs tested, PA was found to most effectively quench the fluorescence emission of the film. When the film was tested in an aqueous solution of a specific NAC (6.0×10^{-5} mol/L), PA

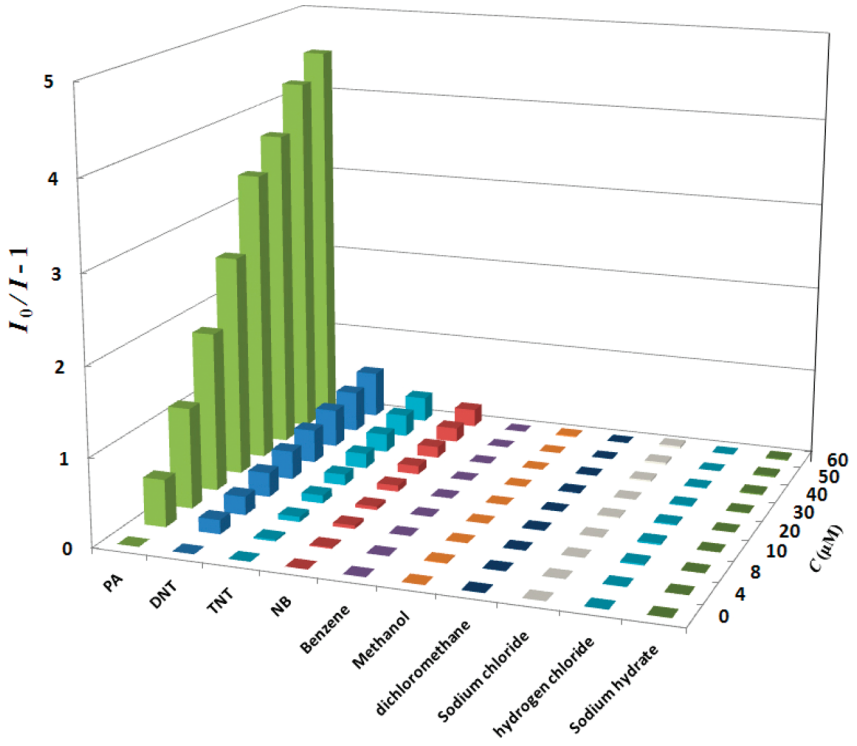

Figure 7. Quenching efficiencies of PA and common interferents to the emission of the film at different concentrations.

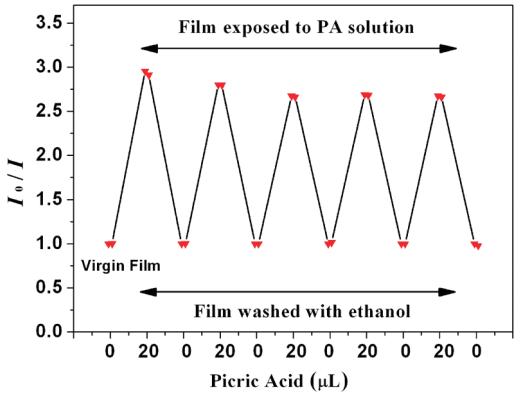

Figure 8. Reversibility of the response of the fluorescent film to PA.

quenched nearly 81.8% of the initial intensity of the film, and furthermore the fluorescence intensity of the film reached a constant value within 90 s after each addition of the quencher solution (c.f. Figure S5 in the Supporting Information). The other aromatics like TNT, DNT, and NB, however, only resulted in some decrease of the fluorescence emission of the film, which is weaker and slower in comparison with PA. Actually, the fluorescence emission of the film decreased significantly with increasing PA concentration (c.f. Figure 5), and the detection limit to PA is found to be about 3.2×10^{-7} mol/L. These results demonstrated that the film has high selectivity and sensitivity to PA when tested in aqueous solution.

The results from lifetime measurements were illustrated in Figure 6. It is obvious that the lifetime of the sensing molecules does not change much along with increasing the concentration of PA. The lifetime ratio, τ_0/τ, is equal to 1, where τ_0 and τ stand for the lifetime of the surface-bound fluorophore in the absence and presence of the quencher, respectively. This phenomenon indicates that the quenching is mainly caused by formation of a nonfluorescent complex in the ground state, which results in electron transfer from the electron-rich fluorophore NA-3T group to the electron-poor analyte PA. So the quenching mechanism of PA to the film was static in nature, as reported previously in other cases.[17−19] Additionally, dynamic quenching studies were initially carried out to characterize the fluorescence quenching efficiencies of these NACs. The Stern−Volmer constant K_{sv} was calculated using the equation of $(I_0/I) = 1 + K_{sv}[A]$, where I_0 and I are the fluorescence intensities of the film before and after adding the quencher, respectively. The value of the constant K_{sv} for PA is about 5.7×10^3 M^{-1}, which is significantly higher than those for other NACs.

The fast response and good selectivity of this NA-3T-functionalized film toward PA make it potential in generating a sensor device to trace amount of PA in aqueous phase. Actually, the reliable detection of trace NACs and NACs related illicit materials has become a focus for preventing terrorist activities and putting a check on their deleterious effects on health.[33−35] However, most of these sensors based on conjugated polymers and oligomers were prepared by spin coating on a solid substrate surface. These methods are only applicable to air samples as a consequence of leaking problems encountered in aqueous media. Even though some reported sensors are capable of detecting explosives in organic solvents, there have been few reported to be used in aqueous medium. For the purpose of practical applications, solid substrate systems that can function in water and humid environment are badly needed.[36,37] The present fluorescent film sensor fabricated by SAM technique has shown better sensing performance as it overcomes all the problem mentioned above. This also suggests the oligothiophene-functionalized films

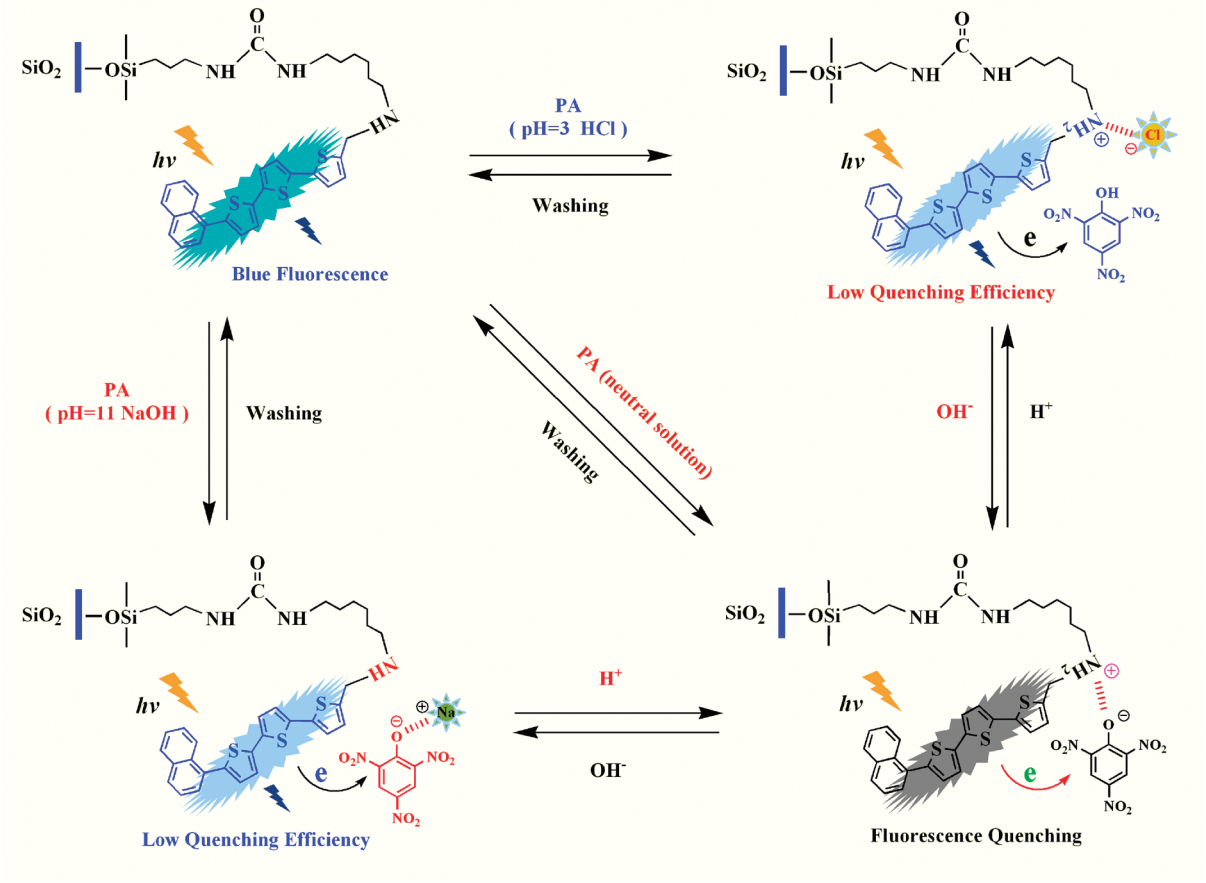

Figure 9. Schematic representation of the electron transfer from NA-3T to PA, and the electrostatic association between PA and the spacer via proton transfer.

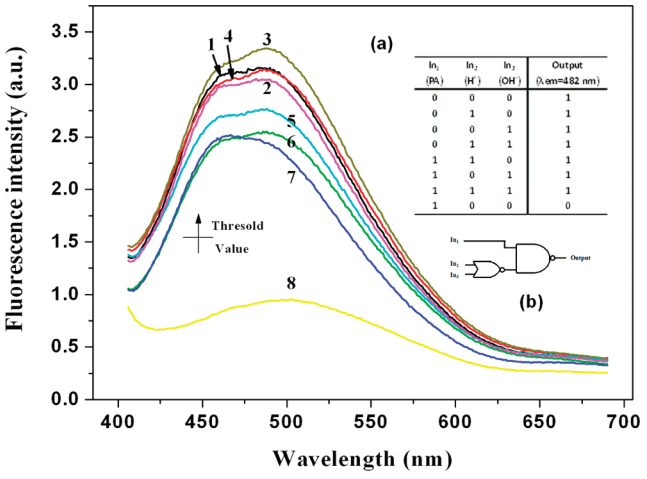

Figure 10. Fluorescence emission spectra of the NA-3T functionalized film recorded at different input conditions: (1) pure water; (2) HCl; (3) NaOH; (4) HCl + NaOH; (5) HCl + PA; (6) HCl + NaOH + PA; (7) PA + NaOH; (8) PA. Fluorescence intensities higher than the threshold value specified at 482 nm (1.5) are assigned as 1 and intensities lower than the value are assigned as 0. The inset is the combinatorial logic scheme.

can explore its function as fluorescent sensing films through our methodology.

3.5. Interference from Other Chemicals. Selectivity and insensitivity to common interferents are important considerations when developing a chemosensor. Figure 7 depicts the plots of $I_0/I - 1$ against the concentration of each NAC and some interferents. Interestingly, no significant change in the fluorescence emission was observed upon exposing the film to common organic solvents such as benzene, methanol, dichloromethane, and the aqueous solutions of NaCl, HCl, or NaOH, revealing that the film is selective to PA.

3.6. Reversibility of the Quenching Process. Reversibility is another important factor determining the usability of a sensing film. The procedures adopted for examination of the reversibility of the sensing process are as follows.[17−19] First, the film was inserted into a cell with 2.5 mL of distilled water, and the fluorescence emission of the film was recorded. Second, 20 μL PA solution (2.5×10^{-3} mol/L) was added, and after 10 min equilibration the fluorescence emission of the film was recorded again. Third, after the measurement, the film was taken out of the cell and rinsed successively with ethanol and distilled water for several times. The results are shown in Figure 8. It is clear that the response of the film to PA is fully reversible, and furthermore, the film is stable, at least, within half a year provided it is properly preserved.

3.7. Quenching Mechanism Studies. It is believed that the fluorescence quenching of the film by NACs presumably involves electron transfer from the excited fluorophore to the LUMO of the explosive materials.[37,38] So the difference between LUMO

energy of the fluorophore and that of the NACs is an important factor in the fluorescence quenching process. With the help of theoretical calculations, the LUMO energy (−2.00 eV) of the fluorophore NA-3T is higher than the LUMO energies of all the NACs detected (PA, −3.90 eV; TNT, −3.49 eV; DNT, −2.97 eV).[29,39] This suggests all the NACs can quench the fluorescence emission of NA-3T. The highest quenching efficiency of PA may come from the electrostatic association between the picrate anion and the protonated amino groups adjacent to NA-3T moieties. It is the association that makes PA have a special affinity to NA-3T and results in a higher quenching efficiency, which is schematically shown in Figure 9.

To confirm the presence of the electrostatic association between the picrate anion and the protonated amino groups in the spacer, a specially designed experiment was conducted. In the experiment, a newly fabricated film was immersed in a HCl solution (pH 3) and the quenching efficiency for PA was measured. It was found that in acidic solution PA shows a much lower quenching efficiency (c.f. Figure S6 in the Supporting Information). This phenomenon may be understood by considering that introduction of HCl brings the system protons, which should be preferentially combined by the amino groups adjacent to the oligothiophenes. In this way, the specific electrostatic association between PA and the spacer is screened, and thereby the quenching efficiency is decreased.

3.8. Fluorescent Logic Gate Studies. In recent years, various logic gates that employ fluorescence changes as outputs have been studied intensively using various inputs, such as pH, metal ions, and anions.[40,41] On the basis of the results demonstrated above, a fluorescence logic gate was established by using PA, proton and hydroxyl ions as independent inputs and by taking fluorescence intensity as output. For the output, the normal fluorescence intensity of the film was defined as 1 and the quenched fluorescence intensity as 0. Herein, 1.5, a value of the fluorescence intensity was taken as the threshold. The output equals 0 when the intensity of the emission at 482 nm is low ($I < 1.5$), whereas the output equals 1 when the intensity of the emission is high ($I > 1.5$). The fluorescence intensities of the film in a PA solution of different pH values are shown in Figure 10 and the results can be explained as follows: (1) in a neutral medium, PA shows the optimum quenching efficiency to the film with the help of the electrostatic association; (2) in an acidic or a basic solution, the quenching efficiency of PA to the film was decreased due to screening of the specific electrostatic association between PA and the spacer as shown in Figure S6 in the Supporting Information and Figure 9, and (3) introduction of both HCl and NaOH (1 to 1 in moles) showed little effect upon the quenching efficiency as shown in Figure 10. The truth table and a schematic representation of the logic gate is shown as an inset of Figure 10. In the circuit, the input data In_2 and In_3 are combined via an NOR operator. The output of the NAND gate is fed by this NOR operator and In_1. Furthermore, the present logic gate could be readily reset by washing the film with pure water, which may guarantee its practical uses.

4. CONCLUSION

Naphthalene was successfully introduced into the conjugated backbone of α-terthiophene, resulting in a new terthiophene derivative, NA-3T, which was further utilized for the fabrication of a monolayer-chemistry-based fluorescent sensing film. Fluorescence measurements demonstrated that unlike α-terthiophene, NA-3T both in solution and in immobilized state exhibits much improved photochemical stability. Utilization of a SAM technique ensures the covalent attachment of NA-3T on the substrate surface and avoids the leaking problem as confronted in spin-coating and other physical methods for preparation of fluorescence sensing films. The present NA-3T-functionalized films as fabricated have shown fast and selective response to PA, with the detection limit being as low as 3.2×10^{-7} mol/L. This great sensitivity to PA has been attributed to the electron transfer from the electron-rich NA-3T group to the electron-poor PA with the help of proton transfer from PA to the amino group in the spacer, which connects the fluorophore to the substrate surface. Interferents such as common organic solvents, acids, and bases show little effect upon the fluorescence emission of the film in aqueous medium. Fluorescence lifetime measurements revealed that the quenching is static in nature. Furthermore, the quenching process is fully reversible. These characteristics showed that the present oliothiophene-functionalized film has great potential in sensing PA. Moreover, the present work has opened a way to fabricate novel fluorescent sensing films by using photochemically stabilized oligothiophene as a new class of sensing elements, which definitely enlarges the applications of oligothiophene, and the space for creating monolayer-chemistry-based fluorescent sensing films.

■ ASSOCIATED CONTENT

Ⓢ Supporting Information. Fluorescence excitation and emission spectra of NTHA in CH_2Cl_2, the detailed calculated data of α-terthiophene and its derivatives, comparison of energy gaps determined by theoretical method and experimental method, fluorescence properties and stability of the NA-3T-functionalized film, time-dependent response of the emission of the film to PA, and the effect of proton on the quenching efficiency of PA to the fluorescent film (PDF). This material is available free of charge via the Internet at http://pubs.acs.org.

■ AUTHOR INFORMATION

Corresponding Author

*E-mail: yfang@snnu.edu.cn (Y.F.); dinglp33@snnu.edu.cn (L.D.). Tel: 0086-29-85310081 (Y.F.) 0086-29-85307534 (L.D.). Fax: 0086-29-85307566 (Y. F.).

■ ACKNOWLEDGMENT

We thank the Ministry of Science and Technology of China (2007AA03Z349), the Natural Science Foundation of China (20927001, 20803046), and the Key Scientific and Technological Innovation Special Projects of Shaanxi "13115" (2010-ZDKG-89) for financial support.

■ REFERENCES

(1) Garcia, P.; Penuut, J. M.; Hapiot, P.; Wiatgens, V.; Vaht, P.; Gander, F.; Dehbouglise, D. *J. Phys. Chem.* **1993**, *97*, 513–516.

(2) Anestopoulos, D.; Fakis, M.; Polyzos, I.; Tsigaridas, G.; Persephonis, P.; Giannetas, V. *J. Phys. Chem. B.* **2005**, *109*, 9476–9481.

(3) Facchetti, A.; Yoon, M. H.; Stern, C. L.; Hutchison, G. R.; Ratner, M. A.; Marks, T. J. *J. Am. Chem. Soc.* **2004**, *126*, 13480–13501.

(4) Kim, D. S.; Ahn, K. H. *J. Org. Chem.* **2008**, *73*, 6831–6834.

(5) Barbarella, G.; Zambianchi, M.; Pudova, O.; Paladini, V.; Ventola, A.; Cipriani, F.; Gigli, G.; Cingolani, R.; Citro, G. *J. Am. Chem. Soc.* **2001**, *123*, 11600–11607.

(6) Batista, R. M. F.; Oliveira, E.; Costa, S. P. G.; Lodeiro, C.; Raposo, M. M. M. *Tetrahedron Lett.* **2008**, *49*, 6575–6578.

(7) Zhang, S.; Cardona, C. M.; Echegoyen, L. *Chem. Commun.* **2006**, *43*, 4461–4473.
(8) Basabe-Desmonts, L.; Reinhoudt, D. N.; Crego-Calama, M. *Chem. Soc. Rev.* **2007**, *36*, 993–1017.
(9) Ding, L.; Fang, Y. *Chem. Soc. Rev.* **2010**, *39*, 4258–4273.
(10) Liu, T. H.; He, G.; Yang, M. N.; Fang, Y. *J. Photochem. Photobiol., A* **2009**, *202*, 178–184.
(11) Liu, T. H.; Nie, Y. X.; He, G.; Zhang, Y.; Ding, L. P.; Fang, Y. *Chem. J. Chin. Univ.* **2010**, *31*, 524–529.
(12) Tian, H. K.; Shi, J. W.; Yan, D. H.; Wang, L. X.; Geng, Y. H.; Wang, F. S. *Adv. Mater.* **2006**, *18*, 2149–2152.
(13) Merlo, J. A.; Newman, C. R.; Gerlach, C. P.; Kelley, T. W.; Muyres, D. V.; Fritz, S. E.; Toney, M. F.; Frisbie, C. D. *J. Am. Chem. Soc.* **2005**, *127*, 3997–4009.
(14) Barbarella, G.; Pudova, O.; Arbizzani, C.; Mastragostino, M.; Bongini, A. *J. Org. Chem.* **1998**, *63*, 1742–1745.
(15) Wiirthner, F.; Vollmer, M. S.; Effenberger, F.; Emele, P.; Meyer, D. U.; Port, H.; Wolf, H. C. *J. Am. Chem. Soc.* **1995**, *117*, 8090–8099.
(16) Wong, K. T.; Wang, C. F.; Chou, C. H.; Su, Y. O.; Lee, G. H.; Peng, S. M. *Org. Lett.* **2002**, *4*, 4439–4442.
(17) Zhang, S. J.; Lü, F. T.; Gao, L. N.; Ding, L. P.; Fang, Y. *Langmuir* **2007**, *23*, 1584–1590.
(18) He, G.; Peng, H. N.; Liu, T. H.; Yang, M. N.; Zhang, Y.; Fang, Y. *J. Mater. Chem.* **2009**, *19*, 7347–7353.
(19) Lü, F. T.; Gao, L. N.; Ding, L. P.; Jiang, L. L.; Fang, Y. *Langmuir* **2006**, *22*, 841–845.
(20) Kuroda, M.; Nakayama, J.; Hoshino, M. *Tetrahedron* **1993**, *49*, 3735–3748.
(21) Anestopoulos, D.; Fakis, M.; Polyzos, I.; Tsigaridas, G.; Persephonis, P.; Giannetas, V. *J. Phys. Chem. B* **2005**, *109*, 9476–9481.
(22) Xie, Y.; Geng, L. N.; Qu, F.; Luo, A. Q.; Qu, F.; Deng, Y. L. *Chin. Sci. Bull.* **2009**, *54*, 738–742.
(23) Delorme, N.; Bardeau, J.-F.; Bulou, A.; Poncin-Epaillard, F. *Langmuir* **2005**, *21*, 12278–12282.
(24) Ulman, A. *Chem. Rev.* **1996**, *96*, 1533–1554.
(25) Lü, F. T.; Gao, L. N.; Li, H. H.; Ding, L. P.; Fang, Y. *Appl. Surf. Sci.* **2007**, *253*, 4123–4131.
(26) Hamai, S. *Bull. Chem. Soc. Jpn.* **1998**, *71*, 1549–1554.
(27) Melo, J. S.; Silva, L. M.; Kuroda, M. *J. Chem. Phys.* **2001**, *115*, 5625–5636.
(28) Pina, J.; Melo, J. S. S. *Phys. Chem. Chem. Phys.* **2009**, *11*, 8706–8713.
(29) Sanchez, J. C.; DiPasquale, A. G.; Rheingold, A. L.; Trogler, W. C. *Chem. Mater.* **2007**, *19*, 6459–6470.
(30) Li, Z. F.; Pei, J. N.; Li, Y. W.; Xu, B.; Deng, M.; Liu, Z. Y.; Li, H.; Lu, H. G.; Li, Q.; Tian, W. J. *J. Phys. Chem. C* **2010**, *114*, 18270–18278.
(31) Leeuw, D. M.; Simenon, M. M. J.; Einhard, R. E. F. *Synth. Met.* **1997**, *87*, 53–59.
(32) Thompson, B. C.; Kim, Y. G.; Reynolds, J. R. *Macromolecules* **2005**, *38*, 5359–5362.
(33) Hu, Y. J.; Tan, S. Z.; Shen, G. L; Yu, R. Q. *Anal. Chim. Acta* **2006**, *570*, 170–175.
(34) Suman, S. *J. Hazard. Mater.* **2007**, *144*, 15–28.
(35) Basabe-Desmonts, L.; Reinhoudt, D. N.; Crego-Calama, M. *Chem. Soc. Rev.* **2007**, *36*, 993–1017.
(36) Lu, P.; Lam, J. W. Y.; Liu, J. Z.; Jim, C. K. W.; Yuan, W. Z.; Xie, N.; Zhong, Y. C.; Hu, Q.; Wong, K. S.; Cheuk, K. K. L.; Tang, B. Z. *Macromol. Rapid Commun.* **2010**, *31*, 834–839.
(37) Sohn, H.; Calhoun, R. M.; Sailor, M. J.; Trogler, W. C. *Angew. Chem., Int. Ed.* **2001**, *40*, 2104–2105.
(38) Toal, S. J.; Trogler, W. C. *J. Mater. Chem.* **2006**, *16*, 2871–2883.
(39) Türker, L. *J. Hazard. Mater.* **2009**, *169*, 819–823.
(40) Mu, L. X.; Shi, W. S.; She, G. W.; Chang, J. C.; Lee, S. T. *Angew. Chem., Int. Ed.* **2009**, *48*, 3469–3472.
(41) Montenegro, J. M.; Perez-Inestrosa, E.; Collado, D.; Vida, Y.; Suau, R. *Org. Lett.* **2004**, *6*, 2353–2355.